Journal of Nuclear Materials 378 (2008) 327–332

Contents lists available at ScienceDirect

Journal of Nuclear Materials

journal homepage: www.elsevier.com/locate/jnucmat

Very high swelling and embrittlement observed in a Fe–18Cr–10Ni–Ti hexagonal fuel wrapper irradiated in the BOR-60 fast reactor

V.S. Neustroev [a], F.A. Garner [b,*]

[a] Research Institute of Atomic Reactors, Dimitrovgrad, Russia
[b] Pacific Northwest National Laboratory, MS P8-15, P.O. Box 999, Richland WA 99354, USA

ARTICLE INFO

Article history:
Received 15 November 2007
Accepted 23 June 2008

ABSTRACT

The highest void swelling level ever observed in an operating fast reactor component has been found after irradiation in BOR-60 with swelling in Kh18H10T (Fe–18Cr–10Ni–Ti) austenitic steel exceeding 50%. At such high swelling levels the steel has reached a terminal swelling rate of ~1%/dpa after a transient that depends on both dpa rate and irradiation temperature. The transient duration at the higher irradiation temperatures is as small as 10–13 dpa depending on which face was examined. When irradiated in a fast reactor such as BOR-60 with a rather low inlet temperature, most of the swelling occurs above the core center-plane and produces a highly asymmetric swelling loop when plotted vs. dpa. Voids initially harden the alloy but as the swelling level becomes significant the elastic moduli of the alloy decreases strongly with swelling, leading to the consequence that the steel actually softens with increasing swelling. This softening occurs even as the elongation decreases as a result of void linkage during deformation. Finally, the elongation decreases to zero with further increases of swelling. This very brittle failure is known to arise from segregation of nickel to void surfaces which induces a martensitic instability leading to a zero tearing modulus and zero deformation.

Published by Elsevier B.V.

1. Introduction

Currently there is a strong interest in the void swelling behavior of austenitic steels used for the core internals of Western pressurized water reactors (PWRs) and Russian water-cooled, water-moderated energy reactors (VVERs) [1–5]. The primary construction materials of the internals are AISI 304 stainless steel and Kh18H10T (Fe–18Cr–10Ni–Ti) stainless steel, respectively. Void swelling has been raised as a potentially life-limiting phenomenon with respect to license extension of these reactors. In addition to dimensional distortion arising from void swelling and irradiation creep, it is known that swelling at ⩾10% induces a severe form of void-induced embrittlement which raises some safety concerns [6,7].

Of particular interest is the swelling at low temperatures and low dpa rates characteristic of PWR and VVER internals. A number of papers by the authors of the current study have addressed this concern [8–20]. It has been clearly shown for both steels that lower dpa rates decrease the duration of the transient regime of swelling and, therefore, increase swelling at a given exposure level. It has also been convincingly shown that lower dpa rates cause swelling to occur at lower temperatures that encompass all temperatures of relevance to PWR and VVER internals.

Also of interest is the anticipated swelling behavior of the steels at high exposure levels and potentially higher swelling levels associated with life extension. Unfortunately, it is impossible to develop swelling data at very high exposures when irradiation proceeds at relatively low neutron fluxes and correspondingly lower displacement rates. However, it is possible to explore high neutron exposures at PWR and VVER-relevant temperatures using the BOR-60 fast reactor, which has an inlet temperature of 320 °C.

In the current study it is desired to examine whether certain characteristics of swelling observed in AISI 304 stainless steel in the EBR-II fast reactor are also observed in Kh18H10T stainless steel. Of particular interest are the dependence of the transient duration of swelling on temperature and dpa rate, and whether the terminal swelling rate of ~1%/dpa is reached by this steel at high neutron exposures. An additional area of strong interest is the consequences of void swelling on the mechanical properties. This paper addresses these issues by examining a hexagonal wrapper irradiated to rather high swelling levels.

2. Experimental details

A fuel assembly designated O-196 was irradiated without movement or rotation in cell D13 in the third row (13.5 mm from core center) of the BOR-60 fast reactor from December 1983 up to

* Corresponding author. Tel.: +1 509 376 4136; fax: +1 509 376 0418.
E-mail address: frank.garner@pnl.gov (F.A. Garner).

0022-3115/$ - see front matter Published by Elsevier B.V.
doi:10.1016/j.jnucmat.2008.06.036

January 1987. All of its neighbors were fuel assemblies. The flux gradient across the assembly was rather small.

The hexagonal duct served as a wrapper surrounding the fuel assembly and was constructed from a titanium-stabilized Russian stainless steel designated Kh18H10T with nominal composition Fe–18Cr–10Ni–0.5Ti but with a small addition of scandium. This element has been shown in ion and neutron irradiation of pure nickel to strongly retard swelling [21]. The Kh18H10T steel is used in Russian reactors for nuclear applications where AISI 304 would be used in Western reactors. The closest Western analog of the Russian steel is AISI 321 stainless steel. The duct wall was 1 mm thick.

The chemical composition in wt% was measured to be Fe–17.9Cr–10.1Ni–1.22Mn–0.46Ti–0.36Si–0.095C–0.009S–0.032P–0.012N–0.05Sc. The duct was fabricated and then annealed at 800 °C for 2 h, followed by annealing at 600 °C for 1 h.

The temperature and fluence profiles for this duct are shown in Fig. 1. The duct reached a maximum exposure of 12.4×10^{26} n/m^2 ($E > 0.1$ MeV) corresponding to 67 dpa in the BOR-60 neutron spectrum and experienced life-averaged temperatures of 320–620 °C.

When removed from reactor it was obvious from both observation and flat-to-flat measurements that significant volume changes had occurred in this duct. When cutting was employed to produce specimens for examination the duct was observed to be very brittle, with cracking and brittle failure often occurring.

Flat #2 was chosen for the most extensive examination but specimens were cut from all six flats. The duct was sectioned at various elevations to produce specimens of size $5 \times 50 \times 1$ mm on which to perform density measurements using hydrostatic weighing at room temperature in CCl_4 with an accuracy of ±0.2%. A second set of specimens were cut at $55 \times 15 \times 1$ mm to be used for production of tensile specimens. An electro-erosion technique was used to produce a gauge section that was 22.5 mm long, 5.0 mm wide and 1 mm thick. A third set of specimens of $4 \times 4 \times 1$ mm were cut for microscopy examination. Microscopy results were reported earlier by Borodin and coworkers [22].

Twenty-two flat tensile specimens were subjected to tensile tests at a strain rate of 1 mm/min. Tensile tests were conducted at room temperature, a temperature close to the radiation temperature, and also at 800 °C. Some of the tensile results have been presented previously in Russian [23,24].

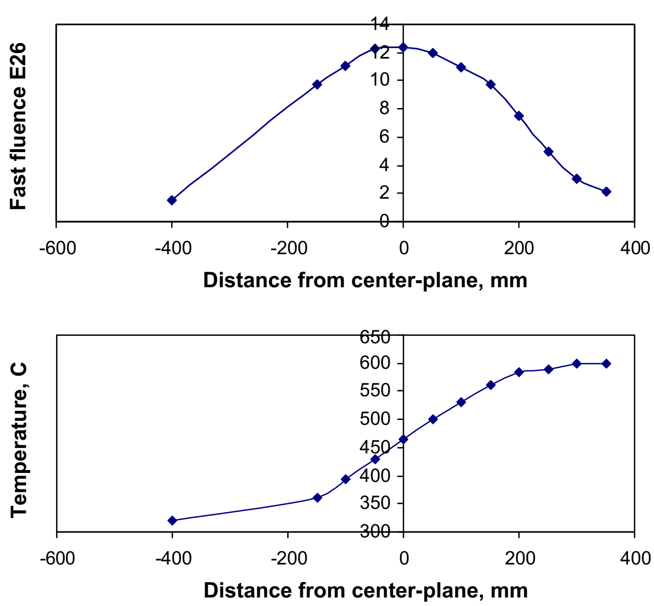

Fig. 1. Calculated fluence and life-averaged temperature distributions along the axis of the wrapper. The temperature cited is the life-averaged value. The fluence quoted is the value above 0.1 MeV in units of 10^{26} n/m^2.

3. Results

3.1. Swelling results

Density change data are presented in Table 1 with all locations being measured from the core center-plane. The faces of the duct were arbitrarily but progressively numbered 1 through 6. The swelling peaked at ~100 mm above the core center-plane on all faces. Note that density changes ($\Delta\rho/\rho_0$) as large as 35.4% were observed with some variations from face-to-face, especially in the high swelling portion of the duct.

However, swelling ($\Delta V/V_0$) in % is defined as $(100\ \Delta\rho/\rho_0)/(100 - \Delta\rho/\rho_0) = 100\ \Delta\rho/\rho_{irr}$. Thus 35.4% density change represents a swelling level of 54.8%. Although relatively large errors are characteristic of microscopy measurements at such high swelling levels, the microscopy measurements by Borodin and coworkers largely confirm the swelling levels measured by density change [22].

Fig. 2 shows the swelling distribution along Flat #2 which peaks at 44.3% at a position 100 mm above the core center-plane. Fig. 3 shows the swelling observed along all six faces, with the peak swelling of 54.8% observed on Flat #1. Note, however, that Flat #1 swells somewhat less than Flat #2 at other elevations.

Looking at the density change data more closely in Fig. 4, however, it appears that Flat #5 actually has the largest overall swelling, perhaps as large as ~60%, but a measurement at 100 mm was not made for this duct. The most significant feature of the swelling of the six faces is the face-to-adjacent face continuity of swelling at each elevation, as is also shown in Fig. 4. It appears that face number 5 might be closest to the core centerline, but correlation of peak swelling of individual faces with respect to the core center line could not be made because no record was made of the initial duct orientation and no duct face was specifically marked.

Fig. 5 presents the swelling data of Flat #2 vs. dpa where 10^{26} n/m^2 $E > 0.1$ MeV produces 5.43 dpa. In this presentation the dependence on temperature and dpa rate is manifested as a 'loop' determined by the interaction of the temperature and dpa rate to determine the duration of the transient swelling regime. It is

Table 1
Density changes in % measured on various flats (fast fluence in units of 10^{26} n/m^2 ($E > 0.1$ MeV)

Z, mm	350	300	250	200	150	100	50	0	−50	−100	−150	−400
Fast fluence	2.1	3	5	7.5	9.7	11	12	12.4	12.3	11.1	9.7	1.5
Temp °C	600	600	590	585	560	530	500	465	430	395	360	320
dpa	11.3	16.2	27	40.5	52.4	59.4	64.8	67	66.4	59.9	52.4	8.1
Flat 1	–	–	–	16.8	–	35.4	28.6	–	–	–	–	–
Flat 2	4.8	3.6	10.6	20.4	29.2	30.7	28.2	21.2	9.2	2.3		1.2
Flat 3	3.1	6.7	–	–	27.9	31.2	27.1	24.1	–	–	–	–
Flat 4	1.7	–	–	–	29.2	33.4	26.5	–	6.8	1.5	1.8	–
Flat 5	–	–	–	–	32.3	–	33.8	–	–	–	–	–
Flat 6	–	–	13.2	–	28	–	31.2	–	–	–	–	–

known that the transient regime of swelling in this steel always decreases as the temperature increases from bottom to top of the duct, but increases as the flux increases and then decreases as the flux falls above the core center-plane. Such loops have been observed previously in AISI 304 stainless steel [3].

Each high swelling data point on the flat 2 loop is thought to reside on a separate swelling curve with a swelling rate of ~1%/dpa where the transient duration is complete but was determined by a combination of the dpa rate and temperature. Note that on the high temperature side of the loop a slope of ~1%/dpa is evident, indicating that all temperatures above ~530 °C share the same

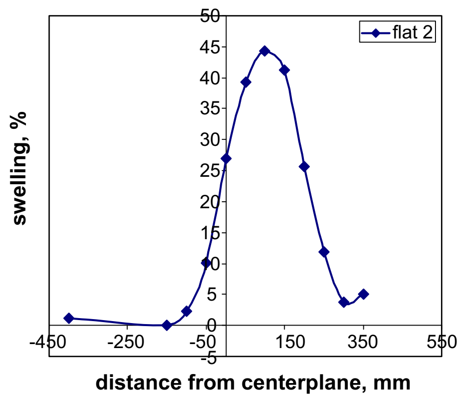

Fig. 2. Swelling observed along the length of Flat #2 of the wrapper.

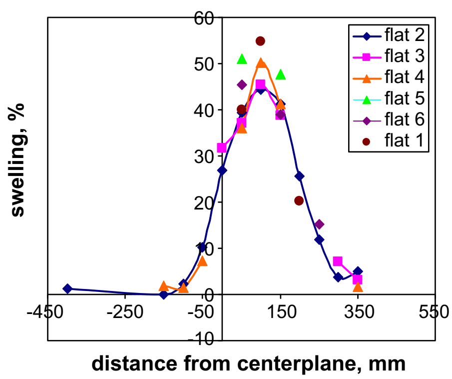

Fig. 3. Swelling observed on all six faces of the wrapper.

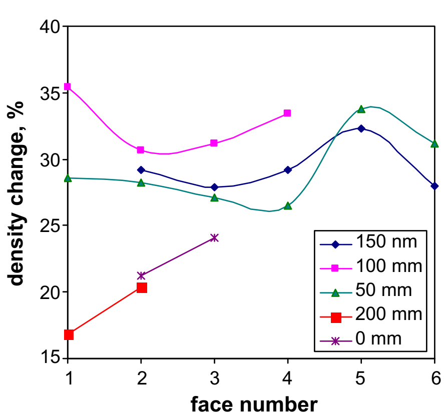

Fig. 4. Continuous swelling variation from face-to-adjacent face at a given elevation, plotting only density values for immediately adjacent faces and only for density changes that are >15%.

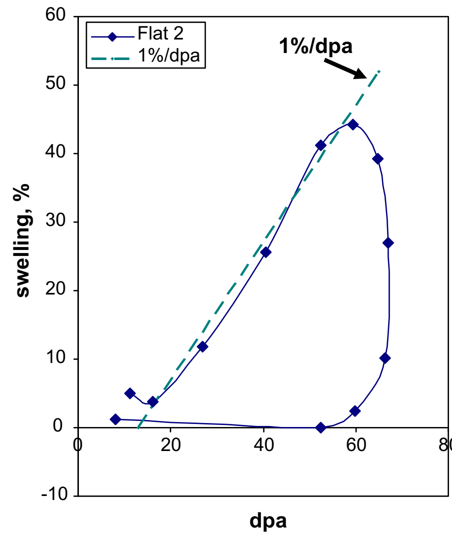

Fig. 5. Swelling plotted vs. dpa level for Flat #2.

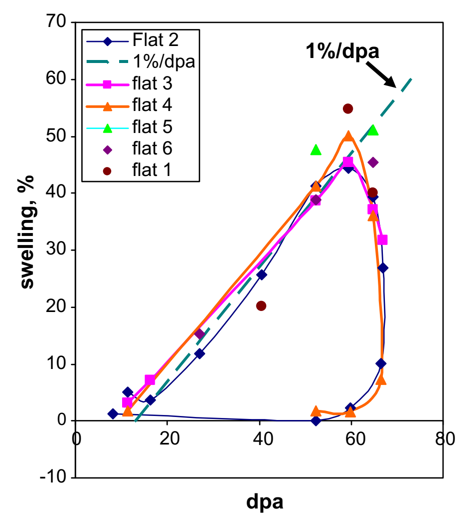

Fig. 6. Swelling plotted vs. dpa level for all flats.

transient duration of ~12 dpa. Fig. 6 shows the swelling of all flats plotted together and reinforces the perception that 1%/dpa is indeed the terminal swelling rate, especially at the higher temperatures. It appears, however, that there may be a slight variation in the transient duration, being somewhat less than 12 dpa on the highest swelling face.

It is interesting to note in the lower-swelling portions of the core, both at lower temperature (0 mm) and higher temperatures (200 mm) the swelling increases from faces 1 to 3, a behavior opposite to that of the higher swelling elevations.

3.2. Mechanical properties

This steel in the annealed, unirradiated state is relatively soft with moderately high ductility. Yield strengths of ~800, 500 and 100 MPa are routinely found when testing at 20, 400 and 800 °C with uniform elongations in the 20–10% range. The results of the post-irradiation tensile tests are shown in Table 2. Fig. 7 presents the results for tests conducted at or near the irradiation temperature.

Note that in three of the test specimens designated numbers 26, 32 and 44, all with rather high swelling levels, failed with

Table 2
Mechanical properties of specimens

Specimen number	Elevation, mm	Swelling, %	Test temp, °C	Ultimate tensile strength, MPa	Yield strength, MPa	Uniform elongation, %	Total elongation, %
14	+250	10.6	590	290	280	0.4	0.4
18	+250	13.2	20	740	610	1.1	1.1
19	+200	16.8	800	75	56	2.5	2.5
27	+150	27.9	20	475	405	0.7	0.7
30	+150	28.0	360	59	–	0	0
29	+150	32.3	500	140	–	0	0
26	+150	29.2	560	0	–	0	0
28	+150	29.2	800	125	110	1.9	3.4
31	+100	35.4	20	138	–	0	0
34	+100	33.4	360	103	–	0	0
32	+100	30.7	530	0	–	0	0
33	+100	31.2	800	31	28	1.6	3.7
37	+50	28.6	20	60	–	0	0
39	+50	27.1	360	141	–	0	0
38	+50	28.2	500	172	–	0	0
40	+50	26.5	590	245	225	1.2	1.2
44	0	21.2	470	0	–	0	0
45	0	24.1	320	482	–	0	0
50	−50	9.2	430	630	610	1.6	1.6
56	−100	2.3	400	765	605	2.0	2.5
62	−150	0	360	825	755	0.7	0.7
68	−400	1.2	800	100	75	11.7	48.6

Specimens 26, 32, 44 failed before testing.

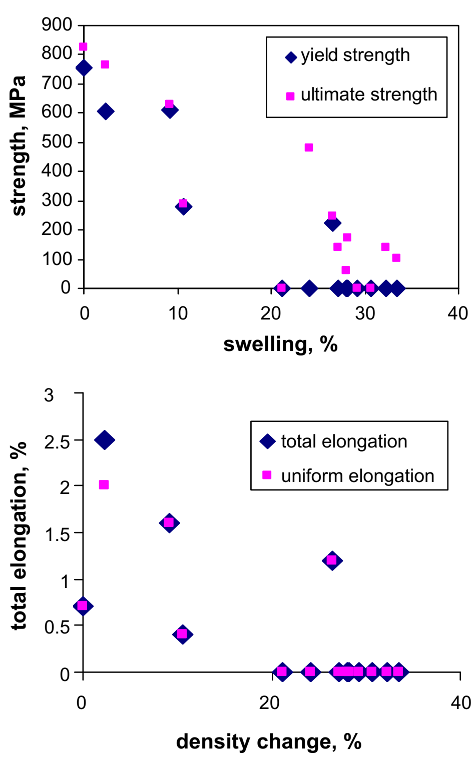

Fig. 7. Mechanical properties of specimens tested at or near the irradiation temperature.

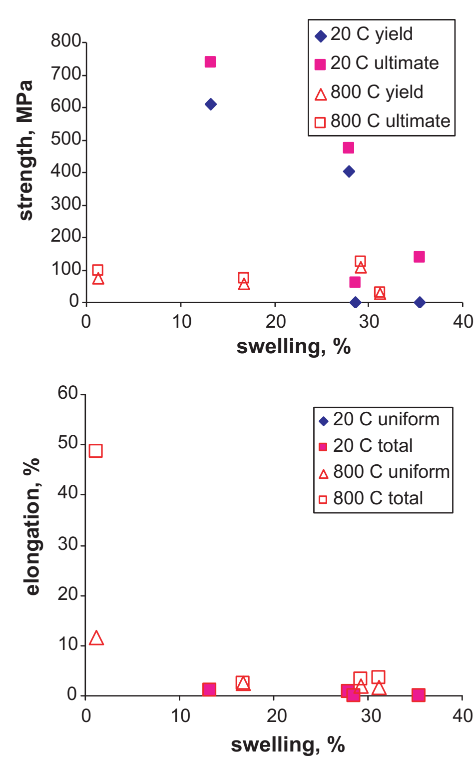

Fig. 8. Mechanical properties observed in tests conducted at 20 °C or 800 °C. Note that uniform and total elongation are equal at 20 °C.

essentially zero elongation before the test was properly started, indicating a very high degree of embrittlement.

Rather than plot the tensile data vs. dpa level, irradiation temperature or test temperature it is instructive to plot the data vs. the swelling level only. Note that as the swelling level reaches and exceeds ~10%, the yield and ultimate strengths have converged. For swelling levels >20% the yield stress and frequently the ultimate stress plunge to zero. It is particularly noteworthy that the steel appears to 'soften' as the swelling increases.

Fig. 8 shows the strength and elongation measurements for tests conducted at 20 and 800 °C. As expected, the strength at 20 °C is somewhat higher than the strength observed at higher test temperatures, and the strength again decreases as swelling increases. In tests conducted at 800 °C the steel is very 'soft' with strengths of ~100 MPa for all swelling levels.

4. Discussion

Although neutron-induced swelling levels of 80–90% have been reached in experimental studies [25,26] the highest swelling level ever reported for a stainless component irradiated in a US fast reactor was ~37% at ~100 dpa in cold-worked D9 [27]. The swelling of 50 to perhaps 60% in the current study is, therefore, the largest reported swelling observed in any fast reactor component.

Based on a large number of earlier studies the higher swelling in Kh18H10T compared to that of D9 probably arises from the combined lack of cold-work, the lower nickel level and especially the pre-irradiation aging treatment employed [28]. It is well-known that aging of most stainless steels at temperatures on the order of 600–800 °C is the surest way to accelerate the onset of swelling [29–33].

It can be seen in Figs. 5 and 6 that the incubation period at the higher irradiation temperatures was only 10–12 dpa, depending on what face was examined. Such aging promotes the early formation of carbide, intermetallic phases and non-equilibrium nickel–silicides such as G-phase, removing elements such as Ni, Si and Ti from solution that tend to resist the onset of swelling. Indeed, Borodin and coworkers found that in this duct large densities of both metal carbides and G-phase were formed with very high nickel (20–73%), silicon (3–25%) and titanium (5–99%) levels. Most interestingly, the scandium introduced into the steel to retard swelling was also concentrated into these precipitates.

The relative continuity of swelling on the various adjacent faces as seen in Fig. 4 confirms that the variations in peak swelling probably arose from face-to-face variations in either temperature or dpa rate rather than as a result of purely random variations in swelling. It was initially assumed that there was not a very significant gradient in neutron flux across the fuel assembly, but this assumption might not be completely accurate to <5%.

In addition, there are always small variations in temperature distribution/history, especially since all neighbors of this assembly were fueled assemblies subject to burn-up and, therefore, experiencing temperature and flux histories of their own. The most likely origin of the face-to-face variations observed probably is related to minor variations in temperature especially.

Fig. 5 demonstrates that all swelling values obtained above ~430 °C lie on swelling curves where the terminal swelling rate of ~1%/dpa has already been reached. Eight of the twelve measurements lie on the above center-plane portion of the duct, where the dpa rates always falling as the temperature increases. The transient duration of swelling in this steel is known to decrease with falling dpa rate and/or increasing temperature [34,35]. AISI 304 stainless steel exhibits the same behavior [36].

When plotted against dpa and ignoring temperature, swelling across components with sufficient swelling in simple steels such as Kh18H10T and AISI 304 stainless steel is seen to develop 'loops' that demonstrate the competitive influence of flux and temperature gradient along the component axis. Fig. 9 shows a previously published example of an annealed AISI 304 loop in an EBR-II hexagonal duct [3]. The EBR-II loop is more symmetric with both low and high temperature sides showing the 1%/dpa tangent.

The Kh18H10T loop is not as symmetric, however, primarily due to the much lower inlet temperature of BOR-60 (330 vs. 370 °C) compared to EBR-II. As a consequence most of the swelling regime on this duct occurs above the core center-plane. Therefore, swelling experiences a continuously declining dpa rate with increasing temperature and produces a rather asymmetric loop, while in EBR-II the swelling regime straddles both increasing and decreasing dpa rates.

When assessing the radiation-induced changes in mechanical properties it is important to realize that most of this duct is dominated by rather high swelling. Although voids initially serve to harden the microstructure [37], large swelling levels allow previously second-order void effects to become dominant [38]. The most consequential of these second-order effects is the strong decrease of elastic moduli at high swelling levels. All of the elastic

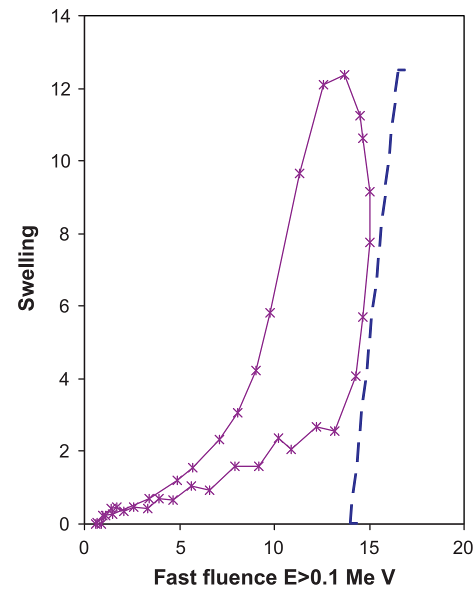

Fig. 9. A swelling loop produced in annealed AISI 304 stainless steel employed as a hexagonal wrapper in EBR-II [3]. Fluences are given in units of 10^{22} n cm^{-2}. The dotted line denotes a swelling rate of 1%/dpa.

moduli are well-known to decrease initially at ~2% per each percent of void swelling [39–43].

As a consequence the slope of the elastic region (Young's modulus) of the stress–strain curve decreases, and more even more importantly the barrier strengths of all sinks decrease as the shear modulus likewise decreases. Therefore, the yield and ultimate strengths decrease with increasing swelling as seen in Figs. 7 and 8, even though the elongation strongly decreases. Similar behavior has also been observed in pure copper [44], but in stainless steels the apparent 'softening' is exacerbated by failure in the elastic region of the stress–strain curve.

The failure mode is strongly influenced by void swelling in two ways. First, crack initiation arising from void-to-void linkage leads to a fracture surface showing extensive ductile dimpling arising from void interactions, a process covered in detail in other recent papers [45,46]. Second, nickel segregation to voids, especially at higher swelling levels, leads to a martensitic instability of the matrix that produces a zero tearing modulus and a fracture surface covered with alpha ferrite [6,47].

Three specimens in this test series failed while loading into the tensile holder and most specimens with >20% swelling appear to have failed by this mechanism. Other high swelling specimens that survived mounting also failed with zero elongation. However, in the current study the failure surface was not examined to confirm the action of the martensite instability.

5. Conclusions

In this study is reported the highest void swelling level ever observed in an operating fast reactor component, exceeding 54 and perhaps reaching ~60% swelling. At very high swelling levels the Kh18H10T steel approaches a terminal swelling rate of ~1%/dpa after a transient that depends on both dpa rate and irradiation temperature. When irradiated in a fast reactor such as BOR-60 with a rather low inlet temperature, most of the swelling occurs above the core center-plane and produces a very asymmetric swelling loop when plotted vs. dpa.

Voids initially harden the matrix, but as the swelling level becomes significant, the elastic moduli decrease strongly, with the consequence that the steel actually softens with increasing swelling, even as the elongation decreases as a result of void linkage during deformation. Finally, zero deformation levels occur at higher swelling levels, arising most likely from a segregation of nickel to void surfaces that induces a martensitic instability and produces a zero tearing modulus.

Acknowledgements

This work was supported by the Russian Science Program of Higher Education, Grant # 2.1.2.7242. The participation of F.A. Garner was supported by the US Department of Energy, Office of Fusion Energy Sciences under Contract DE-AC06-76RLO at Pacific Northwest National Laboratory. PNNL is operated for the Department of Energy by Battelle Memorial Institute.

References

[1] F.A. Garner, L.R. Greenwood, D.L. Harrod, in: Proceedings of the Sixth International Symposium on Environmental Degradation of Materials in Nuclear Power Systems – Water Reactors, San Diego, CA, August 1–5, 1993, p. 783.
[2] F.A. Garner, D.J. Edwards, S.M. Bruemmer, S.I. Porollo, Yu.V. Konobeev, V.S. Neustroev, V.K. Shamardin, A.V. Kozlov, in: Proceedings of the Fontevraud-5, Contribution of Materials Investigation to the Resolution of Problems Encountered in Pressurized Water Reactors, 23–27 September, 2002, Paper #22, on CD Format.
[3] F.A. Garner, B.J. Makenas, in: Fontevraud-6 Symposium on Contribution of Materials Investigations to Improve the Safety and Performance of LWRs, 18–22 September 2006, Fontevraud, France, p. 625.
[4] V.K. Shamardin, V.S. Neustroev, V.I. Prokhorov, et al., in: Proceedings of 5th Russian Conference on Reactor Material Science, Dimitrovgrad, RIAR, vol. 2 (Part 1), 1998, p. 19 (in Russian).
[5] V.S. Neustroev, V.N. Golovanov, V.K. Shamardin, et al., in: Proceedings of 5th Russian Conference on Reactor Material Science Dimitrovgrad RIAR, vol. 3 (Part 1), 2001, p. 3 (in Russian).
[6] M.L. Hamilton, F.H. Huang, W.J.S. Yang, F.A. Garner, in: F.A. Garner, N. Igata, C.H. Henager Jr., (Eds.), Effects of Radiation on Materials: Thirteenth International Symposium (Part II) Influence of Radiation on Material Properties, ASTM STP 956, ASTM Philadelphia, PA, 1987, p. 245.
[7] V.S. Neustroev, V.N. Golovanov, V.K. Shamardin, Atom. Energ. 69 (1990) 223 (in Russian).
[8] F.A. Garner, M.B. Toloczko, J. Nucl. Mater. 251 (1997) 252.
[9] V.S. Neustroev, V.K. Shamardin, Z.E. Ostrovsky, A.M. Pecherin, F.A. Garner, in: M.L. Hamilton, A.S. Kumar, S.T. Rosinski, M.L. Grossbeck (Eds.), Effects of Radiation on Materials: 19th International Symposium, ASTM STP 1366, American Society for Testing and Materials (2000) 792.
[10] F.A. Garner, N.I. Budylkin, Yu.V. Konobeev, S.I. Porollo, V.S. Neustroev, V.K. Shamardin, A.V. Kozlov, in: 11th International Conference on Environmental Degradation of Materials in Nuclear Power Systems – Water Reactors, 2003, p. 647.
[11] F.A. Garner, S.I. Porollo, Yu.V. Konobeev, V.S. Neustroev, O.P. Maksimkin, in: Fontevraud-6 Symposium on Contribution of Materials Investigations to Improve the Safety and Performance of LWRs, 18–22 September 2006, Fontevraud, France, p. 637.
[12] F.A. Garner, S.I. Porollo, A.N. Vorobjev, Yu.V. Konobeev, A.M. Dvoriashin, in: Ninth International Conference on Environmental Degradation of Materials in Nuclear Power Systems – Water Reactors, 1999, p. 1051.
[13] S.I. Porollo, Yu.V. Konobeev, A.M. Dvoraishin, V.M. Krigan, F.A. Garner, in: 10th International Conference on Environmental Degradation of Materials in Nuclear Power Systems – Water Reactors, 2001 (Issued on CD format).
[14] S.I. Porollo, Yu.V. Konobeev, A.M. Dvoriashin, A.N. Vorobjev, V.M. Krigan, F.A. Garner, J. Nucl. Mater. 307–311 (2002) 339.
[15] N.I. Budylkin, T.M. Bulanova, E.G. Mironova, N.M. Mitrofanova, S.I. Porollo, V.M. Chernov, V.K. Shamardin, F.A. Garner, J. Nucl. Mater. 329–333 (2004) 621.
[16] S.I. Porollo, Yu.V. Konobeev, A.M. Dvoriashin, V.M. Krigan, F.A. Garner, in: M.L. Grossbeck, T.R. Allen, R.G. Lott, A.S. Kumar (Eds.), Effects of Radiation on Materials ASTM STP 1447, ASTM International, West Conshohocken PA, 2004, p. 429.
[17] S.I. Porollo, A.M. Dvoriashin, Yu.V. Konobeev, A.A. Ivanov, S.V. Shulepin, F.A. Garner, J. Nucl. Mater. 359 (2006) 41.
[18] F.A. Garner, S.I. Porollo, Yu.V. Konobeev, O.P. Maksimkin, in: Proceedings of 12th International Conference on Environmental Degradation of Materials in Nuclear Power Systems – Water Reactors, 2005, p. 439.
[19] O.P. Maksimkin, K.V. Tsai, L.G. Turubarova, T.A. Doronina, F.A. Garner, J. Nucl. Mater. 367–370 (2007) 990.
[20] O.P. Maksimkin, K.V. Tsai, L.G. Turubarova, T. Doronina, F.A. Garner, J. Nucl. Mater. 329–333 (2004) 625.
[21] V.S. Neustroev, V.K. Shamardin, L.S. Ozigov, in: Voprosy Atomnoy Nauki i Tehniki. Seria: Fizika Radiatsionnyh Povregdeniy i Radiatsionnoe Materialovedenie, Issue 1(73), 2(74), Kharkov, 1999, p. 107 (in Russian).
[22] O.V. Borodin, V.V. Bryk, V.V. Voyevodin, I.M. Neklyudov, V.K. Shamardin, V.S. Neustroev, in: Effects of Radiation on Materials: 17th International Symposium, ASTM STP 1270, 1996, p. 817.
[23] V.S. Neustroev, V.K. Shamardin, Phys. Met. Metall. 83 (5) (1997) 555 (Russian).
[24] V.S. Neustroev, V.K. Shamardin, Atom. Energ. 71 (4) (1991) 345 (in Russian).
[25] F.A. Garner, D.S. Gelles, in: N.H. Packan, R.E. Stoller, A.S. Kumar (Eds.), Proceedings of Symposium on Effects of Radiation on Materials: 14th International Symposium, ASTM STP 1046, vol. II, American Society for Testing and Materials, Philadelphia, 1990, p. 673.
[26] F.A. Garner, J. Nucl. Mater. 122 & 123 (1984) 459.
[27] B.J. Makenas, S.A. Chastain, B.C. Gnieting, in: ANS Winter Meeting on LMR: A Decade of LMR Progress and Promise, 1990, p. 176.
[28] F.A. Garner, Vol. 10A of Materials Science and Technology: A Comprehensive Treatment, VCH Publishers, 1994. p. 419.
[29] H.R. Brager, F.A. Garner, Trans. ANS 28 (1978) 151.
[30] F.A. Garner, J.F. Bates, M.A. Mitchell, J. Nucl. Mater. 189 (1992) 201.
[31] H.J. Busboom, G.C. McClellan, W.L. Bell, W.K. Appleby, Swelling of Types 304 and 316 Stainless Steel Irradiated to $8 \times 1022\,n/cm^2$, General Electric Company Report GEAP-14062, Sunnyvale CA, 1975.
[32] V.A. Krasnoselov, V.I. Prokhorov, A.N. Kolesnikov, Z.A. Ostrovskii, Atom. Energ. 54 (2) (1983) 111 (in Russian).
[33] K. Erhlich, A. Calza Bini, V. Levy, C. Brown, M. Lippens, in: Proceedings of International Conference on Reliable Fuels for Liquid Metal Reactors, Tucson, ANS, 1986, p. 4-1.
[34] T. Okita, N. Sekimura, T. Sato, F.A. Garner, L.R. Greenwood, J. Nucl. Mater. 307–311 (2002) 322.
[35] T. Okita, N. Sekimura, F.A. Garner, L.R. Greenwood, W.G. Wolfer, Y. Isobe, in: 10th International Conference on Environmental Degradation of Materials in Nuclear Power Systems – Water Reactors, 2001 (Issued on CD format).
[36] F.A. Garner, D.L. Porter, in: Proceedings International Conference on Dimensional Stability and Mechanical Behavior of Irradiated Metals and Alloys, April 11–13, vol. II, Brighton, England, 1983, p. 41.
[37] F.A. Garner, M.L. Hamilton, N.F. Panayotou, G.D. Johnson, J. Nucl. Mater. 103 & 104 (1981) 803.
[38] F.A. Garner, M.B. Toloczko, J. Nucl. Mater. 206 (1993) 230.
[39] J.L. Straalsund, C.K. Day, Nucl. Technol. 20 (1973) 27.
[40] M. Marlowe, W.K. Appleby, Trans. ANS 16 (1973) 95–96.
[41] R.L. Trantow, Ultrasonic Measurement of Elastic Properties in Irradiated 304 Stainless Steel, Hanford Engineering Development Laboratory Report HEDL-TME-73-92, 1973.
[42] I.I. Balachov, F.A. Garner, Y. Isobe, M. Sagisaka, H.T. Tang, in: 11th International Conference on Environmental Degradation of Materials in Nuclear Power Systems – Water Reactors, 2003, p. 640.
[43] I.I. Balachov, E.N. Shcherbakov, A.V. Kozlov, I.A. Portnykh, F.A. Garner, J. Nucl. Mater. 329–333 (2004) 617.
[44] K.R. Anderson, F.A. Garner, M.L. Hamilton, J.F. Stubbins, in: R.E. Stoller, A.S. Kumar, D.S. Gelles (Eds.), Proceedings 15th International Symposium on the Effects of Radiation on Materials, ASTM STP 1125, 1992, p. 854.
[45] V.S. Neustroev, in: Proceedings of 8th Russian Conference on Reactor Material Science, Dimitrovgrad, RIAR, in press (in Russian).
[46] V.S. Neustroev, F.A. Garner, in: Proceedings of ICFRM-13, J. Nucl. Mater., in press.
[47] V. Shcherbak, V.D. Dimitryev, Fiz. Met. Metallovid. 6 (1987) 592.